Submitted to Journal of Materials Research and Technology

Hardness evolution of AZ80 magnesium alloy processed by HPT at different temperatures

Saad A. Alsubaie[1,*], Yi Huang[1,*], Terence G. Langdon[1]

[1] Materials Research Group, Faculty of Engineering and the Environment, University of Southampton, Southampton SO17 1BJ, U.K.

[*]Corresponding author: Tel: + 44-23-8059 3766
E-mail: y.huang@soton.ac.uk (Yi Huang), saa1a12@soton.ac.uk (Saad A. Alsubaie)

Abstract

Discs of an extruded AZ80 magnesium alloy were processed by high-pressure torsion (HPT) using 6.0 GPa up to 10 turns at different temperatures (296 K and 473 K). The disc surfaces and cross-sectional planes were examined before and after processing using optical microscopy and Vickers microhardness (Hv). The microhardness results at the surface show differences in the strength of the material as a function of distance from the disc centres up to saturation, as well as a function of distance from the bottom to the surface in the cross-sectional plane. This study analyses the effect of processing temperature on the evolution of microhardness of AZ80 magnesium alloy processed by high-pressure torsion.

Keywords: Hardness; High-pressure torsion; Magnesium alloy; Severe plastic deformation.

1. Introduction

It is well established that grain size has a great influence on the strength of magnesium alloys based on the Hall-Petch relationship [1,2]. By decreasing the grain size to the nanometer scale, the microhardness values (Hv) of magnesium alloy can be increased by a factor of two [3]. Severe plastic deformation (SPD) is well known as an effective process in refining the grain size of metals and alloys to the nanometer range [4]. Several techniques have been presented as SPD methods, such as accumulative roll-bonding [5], twist extrusion [6] and friction stir processing [7], but the most common methods are equal-channel angular pressing (ECAP) [8] and high-pressure torsion (HPT) [9].

Interest in magnesium alloy has increased in recent years due to its high specific strength and low density compared to other structural metals and alloys. Weight reduction is an important factor in fuel economy, so magnesium alloys are attractive for use in the transport industry [10], for example the selection of AZ80 magnesium alloy as a candidate for the structural frames of electrical buses [11]. As a consequence of its hexagonal close-packed (HCP) crystal structure and limited slip systems, magnesium alloy lacks ductility at ambient temperatures [12]. At room temperature, deformation can be achieved by two dominant mechanisms: slip in the basal plane and mechanical twinning [13,14]. Magnesium alloy has three slip systems in the basal plane, of which two are independent, but in order to achieve homogenous deformation without cracks developing, five independent slip systems are required, according to von Mises' criteria. For this reason, the homogenous deformation of magnesium at room temperature without cracking is difficult, and limits its use in many applications.

HPT processing has proved a successful method in processing difficult-to-work alloys such as magnesium alloy AZ31 [15] AZ80 [16] and AZ91 [17] at low temperatures, due to the imposition of extensive hydrostatic pressure during the process. However, variation in the imposed strain in the HPT process depends on distance from the disc centre, based on the equivalent von Mises strain, ε_{eq}, given by the following relationship [18,19]

$$\varepsilon_{eq} = \frac{2\pi N r}{h\sqrt{3}} \tag{1}$$

where *N* is the number of HPT revolutions and *r* and *h* are the radius and height (or thickness) of the disc. It can be seen from Eq. (1) that the larger the displacement from the centre, the greater the imposed strain. This lack of homogeneity in strain induced along the disc diameter can be eliminated by increasing the number of HPT turns [20,21],

Investigation of microhardness evolution can provide a good understanding of microstructure evolution. Recording and analysis of microhardness values across the disc diameter have been a main prompts to study the evolution of the material's microstructure [9,22].

In this investigation, the microhardness evolution of AZ80 magnesium alloy processed by HPT at 296 K and 473 K was examined at the disc surface and through the disc thickness. To date, there is a lack of information about AZ80 magnesium alloy processed by HPT at either room temperature or at an elevated temperature. In this study, HPT processing was conducted at both, using an applied pressure of 6.0 GPa.

2. Experimental material and procedures

A commercial AZ80 magnesium alloy (Mg-8.7% Al-0.51% Zn) was used in this investigation, supplied by Magnesium Electron Ltd (Swinton, Manchester, UK) as extruded rod with a diameter of 9.6 mm.

The microstructure in the as-received condition was investigated using scanning electron microscopy (SEM). After HPT, measurements were taken to determine the Vickers microhardness, Hv, across the surface of the discs and through the thickness of the discs.

The initial microhardness values (Hv) was ~ 63 in the as-received condition and the initial average grain size was ~25 μm [16]. Thin discs were sliced from the extruded rod of a thickness of ~1.5 mm and subsequently ground with an abrasive paper to a thickness of ~0.85 mm.

These discs were processed by HPT under quasi-constrained conditions [23] by a specified number of turns (N), namely 0, 1/4, 1, 3, 5 and 10. Using an applied pressure of 6.0 GPa and a rotation speed of 1 rpm, for each number of turns in the HPT process the discs were processed at two different temperatures, 296 K and 473 K. The higher temperature of 473 K was achieved using a heating element attached to the upper and lower anvil. The temperature of the process was measured continuously through a thermocouple positioned in the upper anvil. Before processing at elevated temperature the required temperature was held for 10 minutes before HPT processing, while a sample was placed in the lower cavity to achieve homogenous temperature distribution between the anvils and the samples.

Following HPT, the discs were cold-mounted, ground and polished. The Vickers microhardness, Hv, was recorded along the diameter and across the whole surface of the discs using an applied load of 100 gf and a dwell time for each measurement of 15 s, following a similar procedure described in detail in an earlier report [24]. Discs were investigated through their thickness using three selected discs processed for N = 1, 3 and 10 turns. The investigation through the discs' thickness using an applied loads of 100 gf and a dwell time of 10 s has been described earlier [25].

3. Experimental results

The AZ80 magnesium alloy was examined in its initial condition using SEM. First, an inspection of the unprocessed disc shown fairly equiaxed grains and a uniform structure. This homogeneity in the microstructure at the surface of the material was demonstrated by the distribution of microhardness values and the average grain size distribution across the entire disc surface [16]. As shown in Fig. 1, the microstructure of the extruded AZ80 has two phases: the α matrix, and the β phase ($Mg_{17}Al_{12}$ precipitate) that is rich in aluminum. The β phase was found to be

widespread discontinuously at the grain boundaries in agglomerate form, as shown in the SEM image in Fig. 1(b).

The microhardness values, Hv, are plotted individually for each processed turn at 296 K and 473 K. Fig. 2 illustrates the results for: (a) N = 0; (b) N = ¼; (c) N = 1; (d) N = 3; (e) N = 5; and (f) N = 10. For all numbers of turns, the microhardness values of samples processed at 296 K are higher than the microhardness values of samples processed at 473 K. There was an overlap in some areas of the discs processed for fewer numbers of turns, as shown in Fig. 2(a), (b) and (c). The microhardness values of discs processed at 473 K are higher in those areas than the values of samples processed at 296 K. It is clear that the peripheries of the discs have higher microhardness values than the centres. In discs processed for ¼ turn, the microhardness values were ~110 Hv at the edge and ~85 Hv at the centre, and ~105 Hv at the edge and ~85 Hv at the centre for temperatures of 296 K and 473 K respectively. After 3 turns, the gap between the microhardness values of the two temperatures became larger, favouring the samples processed at room temperature. The variation in values between the edge and the centre of the disc seemed to be less in discs processed at an elevated temperature. There was a gradual increase in microhardness values from the discs' periphery towards the centre with increasing numbers of turns. Thus, microhardness values become more homogenous along the disc diameter after 5 turns.

Fig. 3 shows the hardness evolution occurring during the HPT process at the centre and the edges of the discs for all number of HPT process turns at both processing temperatures. The microhardness values at the centre and at the edge of the discs were plotted against the number of HPT turns. The increase in microhardness values from the as-received condition at both the centre and the disc edge started at the pressing stage, which indicates the participation of the compression stage of HPT in the hardness evolution of the alloy. There was a slight difference in the microhardness values between the centre and the edge of the disc at both temperatures, the difference being somewhat greater in the samples processed at room temperature than in the samples processed at an elevated temperature. When the alloy was processed for 5 turns at temperatures of either 296 K or 473 K it showed reasonable homogeneity and the difference in values between the centre and the edge of the disc became very small. This behaviour continued up to 10 turns of the HPT process, demonstrating a saturation level of microhardness values between 5 and 10 turns of HPT process at each temperature.

The microhardness values across the whole surface of the disc processed by HPT for 1/4 and 5 turns were recorded using a rectilinear grid pattern, with 0.3 mm spacing between points across the whole surface of the disc. Fig. 4 was generated by plotting those values against their frequency. The average microhardness values in this histogram are represented by vertical lines. At the 298 K, as shown in Fig. 4(a) and (c), the recorded values at 1/4 turn extend over a wider range and with increasing number of turns, the range becomes narrower. Furthermore, the average increase in value with increasing number of turns shifted to the right of the graph, where Hv values are higher. In Fig. 4(b) and (d) the histogram shows that the width of the microhardness values does not decrease with increasing number of turns. It is obvious that the values shifted to the side of the graph, as well as the average value, which means increasing the hardness of the alloy with increasing number of turns.

Fig. 5 illustrates the Vickers microhardness, Hv, values through the disc thickness. In samples processed at room temperature, as shown in Fig. 5 (a) and (c), the variation in microhardness values is clearly seen sample at the centre of the disc in the axial direction. Higher values were found in the mid-thickness of the disc. The difference in values between the higher values at the mid-thickness of the disc and the lower values at the bottom or the top surface of the disc decreases with increasing numbers of turns, up to 10 turns. The hardness development in samples processed at an elevated temperature is shown in Fig. 5 (b) and (d). The variation in microhardness values is not significant in discs processed by 1 turn. Higher values were recorded at the disc periphery, with average values of ~105 Hv. The variation between the top and bottom surfaces of the disc was likewise insignificant. In samples processed for 10 turns, there was greater homogeneity of microhardness values in the radial direction than in the axial direction, and the graph shows higher values at the mid-thickness area, with average values of ~120 Hv.

4. Discussion

The microhardness values in this investigation show a gradual evolution towards reasonable homogeneity with increasing numbers of turns of the HPT process at both 296 K and 473 K. The final saturation values of Hv were ~120 and ~110 at 296 K and 473 K respectively, which is almost double the value of the initial condition. Nevertheless, there was a heterogeneity in microhardness values along the disc diameter due to the nature of the imposed strain in the HPT process in the early stages of processing. At this stage, the distribution of microhardness values is not uniform and varies along the diameter of the disc, with lower values at the centre and higher values at the edges of the disc, based on Eq. (1). This behaviour is shown in Fig. 2 (a), (b), (c) and (d) and represents the general model of hardness evolution: the strain hardening model [26]. This type of behaviour is what most metals and alloys reveal, with little or no dynamic recovery [27,28]. The evolution of microhardness values towards the centre of the discs can be explained by the theoretical approach of strain gradient plasticity modelling [29]. As shown in Fig. 2, the differences in Hv values between the centre and the edge of the disc decrease until saturation after 5 turns. This reasonable homogeneity in hardness after 5 turns was predicted, as it has been established by many previous studies [21,30,31].

As shown in Fig. 1 (a) and (b), AZ80 magnesium alloy has a second phase, the β-phase, $Mg_{17}Al_{12}$ in the form of coarse agglomerate discontinuous particles that have an average length of ~ 1-4 μm. It is anticipated that after HPT process the size of the precipitates will be in the nanometer range [32]. These fine particles have a great effect when deforming AZ80 at elevated temperatures, inhibiting grain growth and helping to further grain size reduction [33]. The high Al content (8.7 %) in AZ80 might play an important part in achieving high values of Hv when processing the alloy at elevated temperatures. In contrast with our results, an AZ31 magnesium alloy that has a lower Al content of (3 %) was processed by HPT at 473 K for one and 5 turns in a previous study [34] and it was found that the Hv values after 5 turns of HPT at 473 K were lower than the values recorded after one turn using the same conditions, and attributed to grain growth during the process.

Our results confirmed the heterogeneity of deformation through the disc thickness, with this heterogeneity being more noticeable for discs processed at room temperature than for those processed at an elevated temperature, as shown in Fig.

5. Several studies on various magnesium alloys at room temperature and elevated temperatures demonstrate similar behaviour through the disc thickness [3,17,25]. These results were contrary to the theoretical and experimental expectation of imposed strain based on Eq. 1, which correlates the degree of deformation to the radial distance from the disc centre, but assumes a constant distribution of strain through the disc thickness. Since the high processing temperature (473 K) in HPT fall in the range of recrystallization temperature of magnesium alloy 400–600 K [35], recovery and recrystallization may have contribution to the microstructure and hardness evolution.

5. Summary and conclusions

[1] An AZ80 magnesium alloy was processed by high-pressure torsion for up to 10 turns at 296 K and 473 K.
[2] Processing AZ80 by HPT at 296 K and 473 K up to 10 turns increases the microhardness values to ~120 and ~110 respectively.
[3] The differences in microhardness values between the centre and the periphery of the disc decrease with increasing torsional strain.
[4] The precipitates may play an important part in achieving high microhardness values Hv when processing the alloy by HPT at an elevated temperature.
[5] Less homogeneity appears across the disc thickness after 10 turns of HPT at both 298 and 473 K.

Acknowledgements

This research was presented at the 3rd Pan American Materials Congress held as part of the TMS Annual Meeting in San Diego, California, on February 27 - March 2, 2017. This work was supported by the European Research Council under ERC Grant Agreement No. 267464-SPDMETALS and by the Public Authority for Applied Education and Training (PAAET) in Kuwait.

References

[1] Hall EO. The deformation and aging of mild steel: III Discussion of results. Proc. Phys. Soc. B. 1951;64:747-753.

[2] Petch NJ. The cleavage strength of polycrystals. J. Iron Steel Inst. 1953;174:25-28.

[3] Figueiredo RB, Aguilar MTP, Cetlin PR, Langdon TG. Deformation Heterogeneity on the Cross-Sectional Planes of a Magnesium Alloy Processed by High-Pressure Torsion. Metall. Mater. Trans. A. 2011;42:3013-3021.

[4] Langdon TG. Twenty-five years of ultrafine-grained materials: Achieving exceptional properties through grain refinement. Acta Mater. 2013;61:7035-7059.

[5] Tsuji N, Saito Y, Lee S-H, Minamino Y. ARB (Accumulative Roll-Bonding) and other new Techniques to Produce Bulk Ultrafine Grained Materials. Adv. Eng. Mater. 2003;5:338-344.

[6] Beygelzimer Y, Varyukhin V, Synkov S, Orlov D. Useful properties of twist extrusion Mater. Sci. Eng. A 2009;503:14-17.

[7] Asadi P, Faraji G, Besharati MK. Producing of AZ91/SiC composite by friction stir processing (FSP). Int. J. Adv. Manuf. Technol.2010;51:247-260.

[8] Valiev RZ, Langdon TG. Principles of equal-channel angular pressing as a processing tool for grain refinement. Prog. Mater. Sci. 2006;51:881-981.

[9] Zhilyaev A, Langdon TG. Using high-pressure torsion for metal processing: Fundamentals and applications. Prog. Mater. Sci. 2008;53:893-979.

[10] Aghion E, Bron B, Eliezer D. The role of the magnesium industry in protecting the environment J. Mater. Process. Technol. 2001;117:381-385.

[11] Zhao D, Wang Z, Zuo M, Geng H. Effects of heat treatment on microstructure and mechanical properties of extruded AZ80 magnesium alloy. Mater. Des. 2014;56:589-593.

[12] Mabuchi M, Iwasaki H, Yanase K. Low temperature superplasticity in an AZ91 magnesium alloy processed by ECAE. 1997;36:681-686.

[13] Kainer KU, editor. Magnesium – Alloys and Technology. Germany: Wiley; 2003.

[14] Al-Samman T, Gottstein G. Room temperature formability of a magnesium AZ31 alloy: Examining the role of texture on the deformation mechanisms. Mater. Sci. Eng. A 2008;488:406-414.

[15] Huang Y, Figueiredo RB, Baudin T, Brisset F, Langdon TG. Evolution of strength and homogeneity in a magnesium AZ31 alloy processed by high-pressure torsion at different temperatures. Adv. Eng. Mater. 2012;14:1018-1026.

[16] Alsubaie SA, Bazarnik P, Lewandowska M, Huang Y, Langdon TG. Evolution of microstructure and hardness in AZ80 magnesium alloy processed by high-pressure torsion. J. Mater. Res. Technol. 2016;5:152-158.

[17] Al-Zubaydi A, Figueiredo RB, Huang Y, Langdon TG. Structural and hardness inhomogeneities in Mg–Al–Zn alloys processed by high-pressure torsion. J. Mater. Sci. 2013;48:4661-4670.

[18] Valiev RZ, Ivanisenko YV, Rauch EF, Baudelet B. Structure and deformation behaviour of armco iron subjected to severe plastic deformation. 1996;44:4705-4712.
[19] Wetscher F, Vorhauer A, Stock R, Pippan A. Structural refinement of low alloyed steels during severe plastic deformation. Mater. Sci. Eng. A. 2004;387-389:809-816.
[20] Torbati-Sarraf SA, Langdon TG. Properties of a ZK60 magnesium alloy processed by high-pressure torsion. J. Alloys Compd. 2014;613:357-363.
[21] Xu C, Horita Z, Langdon TG. The evolution of homogeneity in processing by high-pressure torsion. Acta Mater. 2007;55:203-212.
[22] Zhilyaev AP, Oh-ishi K, Langdon TG, McNelley TR. Microstructural evolution in commercial purity aluminum during high-pressure torsion. Mater. Sci. Eng. A. 2005;410-411:277-280.
[23] Hohenwarter A, Bachmaier A, Gludovatz B, Scheriau S, Pippan R. Technical parameters affecting grain refinement by high pressure torsion. Int. J. Mater. Res. 2009;100:1653-1661.
[24] Kawasaki M, Langdon TG. The significance of strain reversals during processing by high-pressure torsion. Mater. Sci. Eng. A. 2008;498:341-348.
[25] Figueiredo RB, Langdon TG. Development of structural heterogeneities in a magnesium alloy processed by high-pressure torsion Mater. Sci. Eng. A. 2011;528:4500-4506.
[26] Kawasaki M, Lee H-J, Ahn B, Zhilyaev AP, Langdon TG. Evolution of hardness in ultrafine-grained metals processed by high-pressure torsion. J. Mater. Res. Technol. 2014;3:311-318.
[27] Kawasaki M. Different models of hardness evolution in ultrafine-grained materials processed by high-pressure torsion. J. Mater. Sci. 2014;49:18-34.
[28] Kawasaki M, Figueiredo RB, Huang Y, Langdon TG. Interpretation of hardness evolution in metals processed by high-pressure torsion. J. Mater. Sci. 2014;49:6586-6596.
[29] Estrin Y, Molotnikov A, Davies DHJ, Lapovok R. Strain gradient modeling of high-pressure torsion. J. Mech. Phys. Solids. 2008;56:1186-1202.
[30] Kawasaki M, Figueiredo RB, Langdon TG. An investigation of hardness homogeneity throughout disks processed by high-pressure torsion. Acta Mater. 2011;59:308-316.
[31] Edalati K, Fujioka T, Horita Z. Evolution of Mechanical Properties and Microstructures with Equivalent Strain in Pure Fe Processed by High Pressure Torsion. Mater. Trans. 2009;50:44-50.
[32] Al-Zubaydi ASJ, Zhilyaev AP, Wang SC, Reed PAS. Superplastic behaviour of AZ91 magnesium alloy processed by high-pressure torsion. Mater. Sci. Eng. A. 2015;637:1-11
[33] Xu SW, Kamado S, Matsumoto N, Honma T, Kojima Y. Recrystallization mechanism of as-cast AZ91 magnesium alloy during hot compressive deformation. Mater. Sci. Eng. A. 2009;527:52-60.
[34] Huang Y, Figueiredo RB, Baudin T, Helbert A-L, Brisset F, Langdon TG. Microstructure and texture evolution in a magnesium alloy during processing by high-pressure torsion. Mater. Res. 2013;16:577-585.

[35] Figueiredo RB, Langdon TG. Grain refinement and mechanical behaviour of a magnesium alloy processed by ECAP. J. Mater. Sci. 2010;45:4827-4836.

Figure captions

Fig. 1 SEM images showing: (a) the grain distribution at the surface of the alloy; and (b) the distribution of the precipitates (Mg_{17} Al_{12}) at the grain boundaries.

Fig. 2 Results of Vickers microhardness values Hv, plotted individually for each number of processed turns at 296 K and 473 K for: (a) N = 0; (b) N = 1/4; (c) N = 1; (d) N = 3, (e) N = 5; and (f) N = 10.

Fig. 3 Comparison of hardness evolution between the centre and the edge of discs processed by HPT for up to 10 turns at: (a) 296 K; and (b) 473 K.

Fig. 4 Histogram of distribution of Vickers microhardness values across the whole disc surface after processing by HPT: (a) and (c) at 296 K, for 1/4 and 5 turns (b) and (d) at 473 K, for 1/4 and 5 turns.

Fig. 5 Microhardness values at different displacements from the centre, as a function of distance from the bottom to the top of discs processed by HPT for: (a) 1 turn at 296 K and (c) 10 turns at 296 K, and for: (b) 1 turn at 473 K; and (d) 10 turns at 473 K.

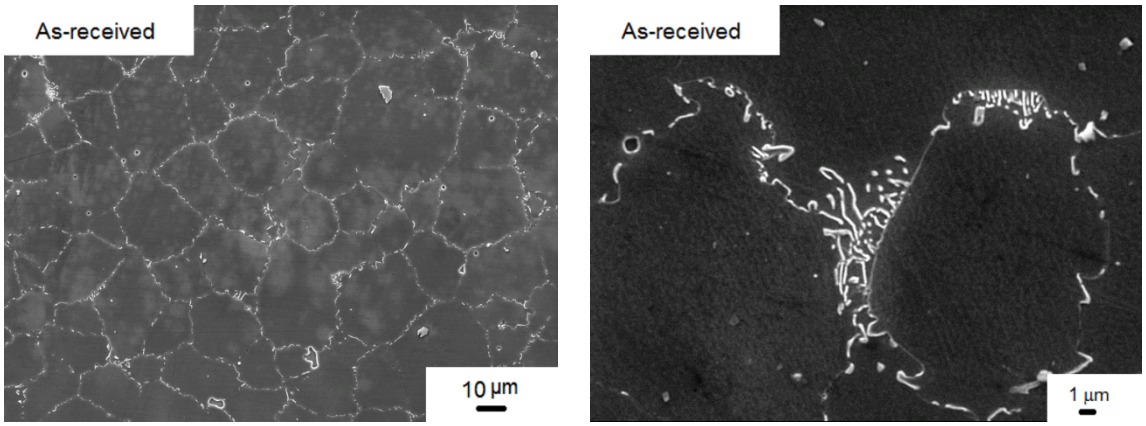

(a) (b)

Fig. 1 SEM images showing: (a) the grain distribution at the surface of the alloy; and (b) the distribution of the precipitates ($Mg_{17}Al_{12}$) at the grain boundaries.

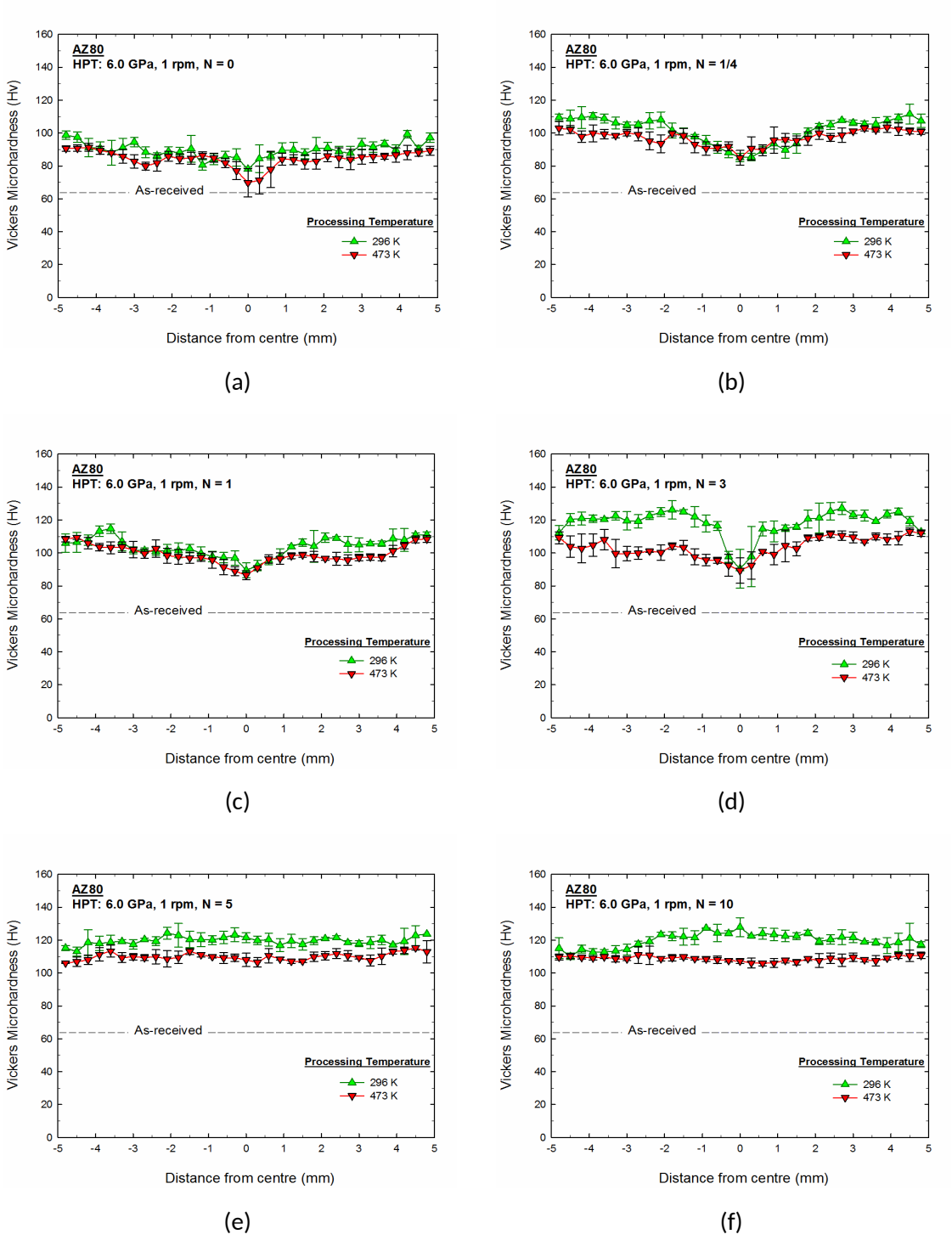

Fig. 2 Results of Vickers microhardness values Hv, plotted individually for each number of processed turns at 296 K and 473 K for: (a) N = 0; (b) N = 1/4; (c) N = 1; (d) N = 3, (e) N = 5; and (f) N = 10.

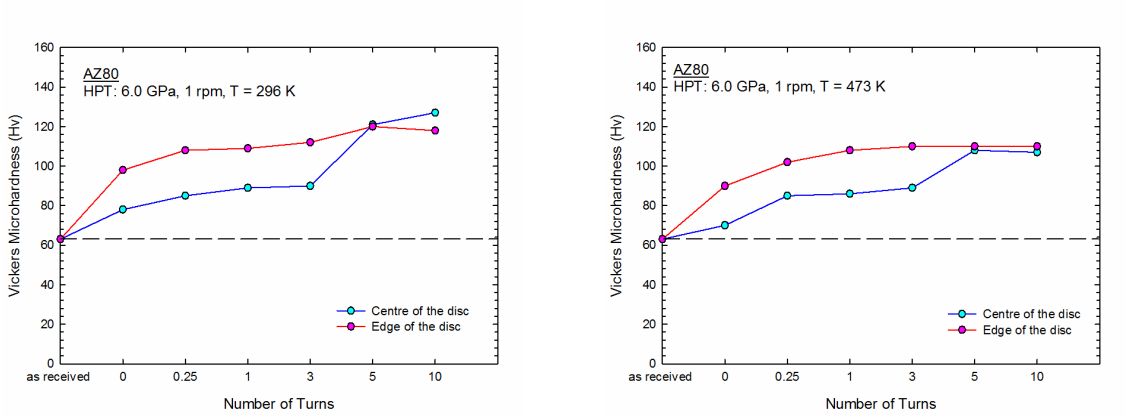

(a) (b)

Fig. 3 Comparison of hardness evolution between the centre and the edge of discs processed by HPT for up to 10 turns at: (a) 296 K; and (b) 473 K.

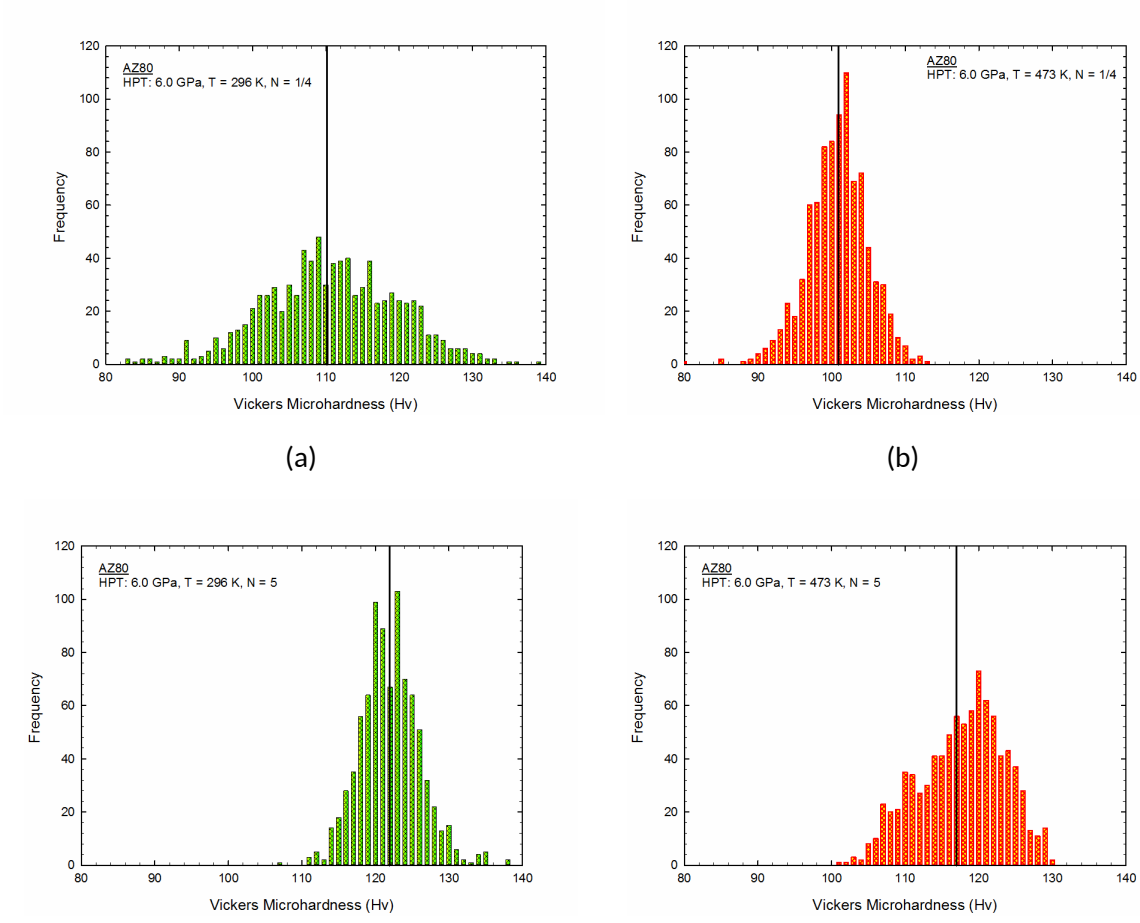

(a) (b)

(c) (d)

Fig. 4 Histogram of distribution of Vickers microhardness values across the whole disc surface after processing by HPT: (a) and (c) at 296 K, for 1/4 and 5 turns (b) and (d) at 473 K, for 1/4 and 5 turns.

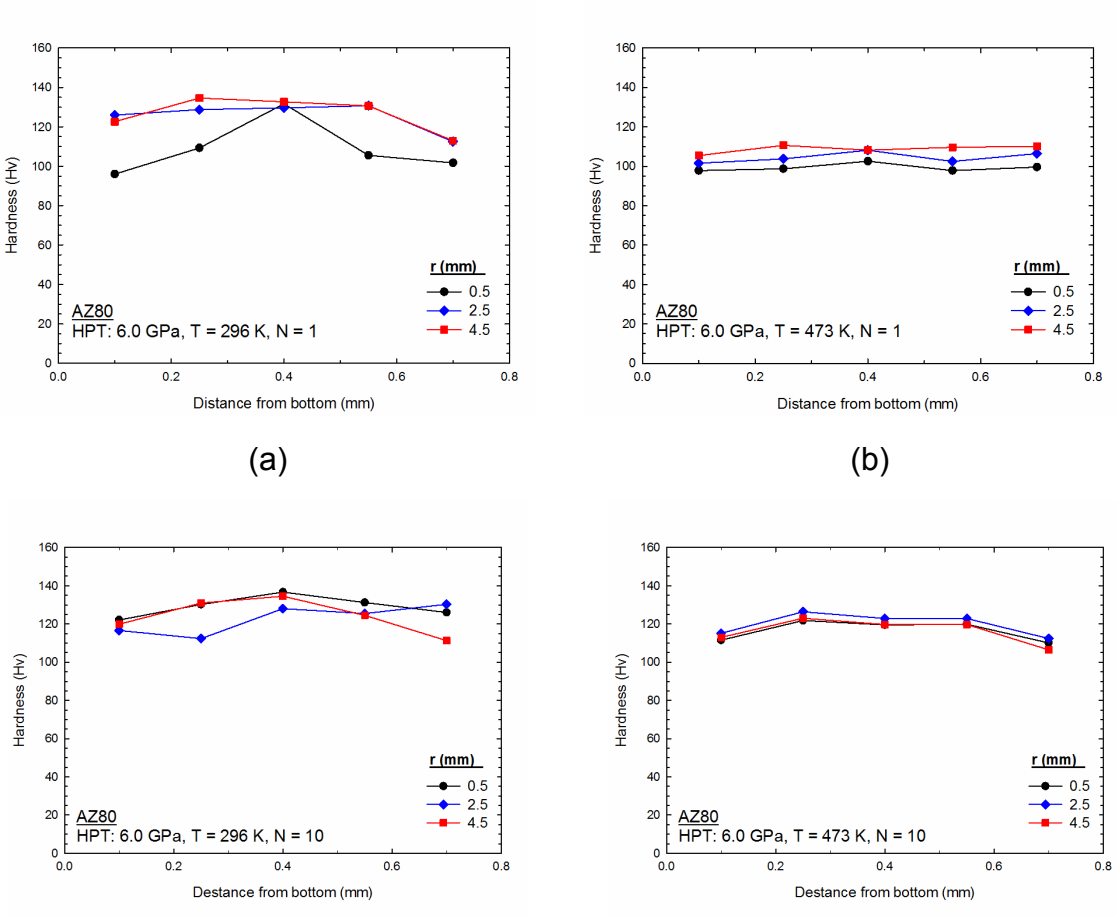

Fig. 5 Microhardness values at different displacements from the centre, as a function of distance from the bottom to the top of discs processed by HPT for: (a) 1 turn at 296 K and (c) 10 turns at 296 K, and for: (b) 1 turn at 473 K; and (d) 10 turns at 473 K.